

Assessment of a 12-story Reinforced Concrete Special Moment Frame Building Using Performance-Based Seismic Engineering Standards and Guidelines: ASCE 41, TBI, and LATBSDC

Mustafa K. Buniya, Andre R. Barbosa, and Siamak Sattar

Synopsis: A 160-foot (≈ 49 m) tall 12-story reinforced concrete special moment frame building is designed following ASCE 7-16 and ACI 318-14, and assessed using three Performance-Based Seismic Engineering (PBSE) standards and guidelines including ASCE/SEI 41, the Tall Buildings Initiative (TBI) guidelines for performance-based design of tall buildings, and the Los Angeles Tall Buildings Structural Design Council (LATBSDC) procedures. The assessments are performed at the combination of two performance and hazard levels including Collapse Prevention (CP) at the risk-targeted maximum considered earthquake (MCE_R) hazard level and Immediate Occupancy (IO) at a frequent ground motion level with 50 percent probability of exceedance in 30 years, *i.e.* serviceability performance level. Based on the recommendations of each of the three PBSE documents, nonlinear finite element models are implemented in OpenSees. Through nonlinear time-history response analyses, the finite element models are subjected to eleven ground motions that are selected following the ground motion selection recommendations in ASCE 7-16. Assessment results indicate that for the serviceability performance level, the code-compliant building meets the design requirements of the three PBSE documents for the interstory drift ratio and inelastic deformation of the structural components. At the MCE_R hazard level, although the building essentially satisfies the design requirements for the peak interstory drift ratios and inelastic deformation, the mean of the residual interstory drift ratios as well as the envelope of the residual drift ratios do not meet the limits of the TBI and LATBSDC guidelines. The results indicate that the newly designed building meets the ASCE 41 acceptance criteria but does not meet the design requirements set in TBI and LATBSDC guidelines.

Keywords: ASCE/SEI 41, LATBSDC, nonlinear modeling, performance-based design, reinforced concrete, special moment frame, TBI

Mustafa K. Buniya is a graduate student in School of Civil and Construction Engineering, Oregon State University, Corvallis, OR. He is on a scholarship program sponsored by the Higher Committee for Education Development in Iraq (HCED). He received his BSCE from University of Anbar, Ramadi, Iraq, and his MSCE from University of Baghdad, Baghdad, Iraq. His research interests include performance-based seismic design of the reinforced concrete buildings.

Andre R. Barbosa is Associate Professor of Structural Engineering at Oregon State University. He received his Ph.D. in Structural Engineering from the University of California San Diego, San Diego, CA in 2011. His research interests include testing and nonlinear modeling of innovative structural materials and structures, performance-based multi-hazard assessment and design, reliability and robustness of structures, and community resilience.

ACI member **Siamak Sattar** is a Research Structural Engineer at the National Institute of Standards and Technology in Gaithersburg, Maryland. He received his Ph.D. in Structural Engineering from University of Colorado-Boulder in 2013. His research is focused on the collapse assessment of reinforced concrete buildings, performance-based seismic design of concrete structures, uncertainty quantification, and ground motion selection.

INTRODUCTION

Interest in implementing Performance-Based Seismic Engineering (PBSE) has grown in the U.S. since the 1990s. Since then, several standards and guidelines have been developed for implementation of PBSE. The three main PBSE standards and guidelines in the United States (US) include the standard for seismic evaluation and retrofit of existing buildings (ASCE/SEI 41-17, 2017), the *Tall Buildings Initiative Guidelines for Performance-based Seismic Design of Tall Buildings* (TBI, 2010), and the *An Alternative Procedure for Seismic Analysis and Design of Tall Buildings Located in the Los Angeles Region* (LATBSDC, 2014) that provide alternative procedures for seismic analysis and design of tall buildings located in Los Angeles, California. Although these three documents target the same goal of regulating the implementation of PBS for practicing engineers, they differ in multiple aspects, including those related to nonlinear structural modeling, analysis procedures, and acceptance criteria used for performance-based seismic design of building structures. In addition to these documents, other efforts have developed guidelines for nonlinear modeling of buildings, including (ACI 374.3R-2016).

Due to the differences mentioned at various levels of the three PBS documents, questions can be raised in terms of what the impact of selecting and implementing different guidelines is on the overall performance assessment and design of buildings, and ultimately whether these guidelines produce safe designs. The PBS documents comparatively target a similar performance objective which is a low probability of collapse at the risk-targeted maximum considered earthquake (MCE_R) hazard level. While all PBS documents target this performance objective, the differences in modeling, analysis, and acceptance criteria among them may imply different probability of collapse for buildings designed per these documents. The challenging issue is how different the margin of safety against collapse, i.e. probability of collapse, would be for buildings designed following different PBS documents. This study is the initial step toward answering this question. Moreover, this study is the first attempt in comparing the design requirements of ASCE 41, TBI, and LATBSDC for reinforced concrete moment frames.

This paper presents a comprehensive review of the ASCE41, TBI, and LATBSDC guidelines for reinforced concrete special moment frames and identifies fundamental differences between these documents. This comparison is made in order to inform practicing engineers and code developers about the differences among these documents, and how one standard may benefit from adopting the design requirements prescribed in a different standard. A 12-story archetype reinforced concrete special moment frame is designed in accordance with the ASCE 7-16 (2016), hereafter known as ASCE 7, and ACI 318-14 (2014) for a far-field site located in Los Angeles, California. The ASCE 7 code-compliant building is then assessed using the three PBSE documents to illustrate differences in terms of seismic performance assessment outcomes. Three-dimensional nonlinear models of the building are developed in the Open System for Earthquake Engineering Simulation (OpenSees, McKenna et al. 2009) following the requirements of each of the three documents. The nonlinear building models are then subjected to a suite of ground motion records scaled to match the MCE_R level and the serviceability level intensity of ground shaking. The deformation demand and the interstory drift ratios are compared against the acceptance criteria set by the PBSE documents. In addition, the comparison of the engineering demand parameters obtained from the nonlinear dynamic response history analyses of the finite element

models developed in accordance with the requirements of the three documents highlights the impact of the modeling assumptions on the performance assessment.

PERFORMANCE OBJECTIVES AND CRITERIA OF ASCE 41, TBI, and LATBSDC

Performance Objectives

The overarching performance objectives of the three documents analyzed herein are described in this section. The performance objective in ASCE 41 for a new building is that the building performs according to ASCE 7's provisions, i.e. Basic Performance Objective Equivalent to New Building Standards (BPN). In this performance objective, a risk category II building shall satisfy Collapse Prevention (CP) at MCE_R and Life-Safety (LS) at $2/3$ of MCE_R . The TBI and LATBSDC performance objectives for a Risk Category II building are: (1) the building shall satisfy Immediate Occupancy (IO) under frequent ground motions with 50 percent probability of exceedance in 30 years (43-year return period), and (2) the building shall have a low probability of collapse under MCE_R shaking. Rather than comparing the acceptance criteria for the performance objectives of each standard individually, this study provides a side-by-side comparison of the criteria for Immediate Occupancy at frequent ground motions (with 50 percent probability of exceedance in 30 years) and Collapse Prevention at the MCE_R .

Modeling Recommendations

The guidelines/standards' recommendations for the performance assessment are fundamentally different in terms of the assignments of material and stiffness properties, and damping ratio. This subsection summarizes the PBSE guidelines recommendations for the modelling and assessment procedures used in this study.

Material, Stiffness Properties, and Damping Ratio— For nonlinear dynamic response history analyses, the structural models should include a realistic estimation of the expected material strengths and stiffnesses. Table 1 summarizes the material over-strength factors used to convert from nominal to expected material strengths provided in each document, where the material over-strength factors are similar for the TBI and LATBSDC, but considerably larger for ASCE 41. In addition to the differences in the expected material strengths, the effective component stiffness to be used in the analyses are also different for the three documents. Table 2 lists the flexural and shear rigidity factors to be used in the analyses as described in each of the three documents. The effective flexural stiffness of columns for ASCE 41 is computed as a function of the level of the applied axial load, while TBI and LATBSDC guidelines suggest fixed values. It can be seen in Table 2 that the shear rigidity factors for ASCE 41 and TBI are similar, while the LATBSDC uses a higher shear rigidity factors and higher flexural rigidity factors for the columns. For the damping ratio, ASCE 41 recommends to use a 5% and 3% as a viscous damping ratio for the serviceability and MCE_R evaluation, respectively. However, in the subsequent application example, a value of 3 % was used in the analysis that is based on the use of nonlinear response history analyses. On the other hand, both the TBI and LATBSDC guidelines recommend the use of a ratio of 2.5% of the critical damping ratio, regardless of the hazard level.

Component Modeling— to develop nonlinear models consistent with the prescriptions of ASCE 41, the modeling parameters for the backbone curves of the plastic hinges of beams and columns are taken from ASCE 41. The ASCE 41 modeling parameters are based on the envelope of the hysteretic response of the moment-rotation hinges. This approach assumes that the cyclic degradation is included in the backbone curve. The TBI and LATBSDC guidelines recommend using one of four options discussed in (ATC-72-1, 2010). In this study, "option 1" of the (ATC-72-1, 2010) modeling recommendations is implemented. This modeling option is based on adopting the monotonic backbone that incorporates cyclic deterioration in the nonlinear response history analyses.

Acceptance Criteria

Table 3 and Table 4 summarize the differences among the three documents in terms of the global acceptance criteria and computation of demand and capacities for the component level check among the three documents when nonlinear dynamic response analysis is used as the analysis procedure for Serviceability and Collapse Prevention performance levels, respectively. ASCE 41 is only explicit about performance acceptance criteria for the component responses associated with the beam and column inelastic rotations. However, ASCE 7 Section 16.2.4.3 requires that, when nonlinear response history analyses are performed, the peak interstory drift ratios cannot exceed 1.25 times of the design peak interstory drift ratio values shown in ASCE 7 Table 12.12.1. It is worth noting that these design values are amplified by 1.5 when performing a performance level assessment corresponding to MCE_R hazard level (Haselton et al. 2017b).

TBI and LATBSDC guidelines recommend checking both building global responses and component responses for both the Collapse Prevention and serviceability performance levels. In terms of global acceptance criteria, for the MCE_R hazard level, TBI and LATBSDC guidelines state that the mean of the peak transient interstory drift ratios over all ground motions used in the analysis should not exceed 3% of the interstory drift at each story. In addition, the guidelines set the peak interstory drift ratios for all stories and over all ground motions to 4.5% of the story heights. In terms of residual drift ratios, TBI and LATBSDC state the mean and envelope of the peak residual drift ratios in each story should not exceed 1.0% and 1.5%, respectively. In addition, TBI and LATBSDC require that no story should lose more than 20% of the initial total story shear strength. For the serviceability performance level, TBI and LATSDC guidelines set that the mean of the interstory drift ratios should not exceed 0.5% in each story.

The computation of demand and capacity for assessment of the performance of the building at the component level varies across the three documents. At the MCE_R hazard level, ASCE 41 allows for the use the mean responses if a minimum of ten ground motions are employed in the analysis. However, TBI requires the use of the maximum responses for deformation-controlled elements, while LATBSDC allows the use of the mean response when at least seven ground motions are employed in the analysis. For the serviceability performance level, the only difference between the three documents is that ASCE 41 allows for the use of the mean response if at least 10 ground motions are used in the analysis, while the TBI and LATBSDC require the use of at least seven ground motions. For the performance level corresponding to MCE_R and serviceability performance level, the CP and IO limits from ASCE 41 can be used as acceptance criteria for all three documents.

BUILDING ARCHETYPE

The performance assessment of a 12-story building archetype is presented for a reinforced concrete special moment frame (SMF) building to be built in a far-field site in Los Angeles, California. The building plan layout and elevation views are illustrated in Fig. 1. This building is designed per ASCE 7 and ACI 318-14. The risk category of the building is II according to ASCE 7, and the building is assumed to be in a site that has a soil class D with an average shear wave velocity V_{s30} of 360 m/s. The spectral response acceleration parameters S_s and S_1 at the site are 1.5g and 0.6g, respectively. The values of the response modification factor R , the system over-strength factor Ω_o , and the deflection amplification factor C_d , for the structural system type are 8.0, 3.0, and 5.5, respectively.

It is assumed that the reinforced concrete is normal weight with 150 pcf (24.0 kN/m³). The nominal compressive strength of concrete used in the design is 5 ksi (34.5 MPa) and 6 ksi (41.4 MPa) for the beams and columns, respectively. The reinforcing steel grade is considered to be ASTM A706 Grade 60 ksi (415 MPa). Slabs are assumed to be 8 in. thick (203 mm) and designed as two-way slabs.

The superimposed dead loads assumed for the design are 10 psf (0.48 kN/m²) for the roof, and for other floors 10 psf (0.48 kN/m²) for ceiling MEP (mechanical, electrical, plumbing), 15 psf (0.72 kN/m²) for partitions, and 15 psf (0.72 kN/m²) for the curtain wall cladding that is supported on perimeter beams. Live loads are assumed to be 30 psf (1.44 kN/m²) and 50 psf (2.39 kN/m²) for roof and floors, respectively. The design load combinations are performed according to the ASCE 7 section 2.3.2 and 12.4.2.3.

For the code-compliant design, a three-dimensional linear elastic computational model was first developed in ETABS (CSI 2013) to compute the force and deformation demands. Masses were computed from weight of each floor and distributed equally to the all nodes at the center of the beam-column joints in the model. The seismic masses consider only the effects of the dead loads and superimposed dead loads according to ASCE 7 section 12.7.2. A rigid diaphragm assumption was considered. The Modal Response Spectrum (MRS) method was used to determine the seismic demands on the columns and beams, with the scaling required such that the MRS base shear is at least equal to the equivalent lateral force (ELF) determined seismic demands per recommendations in the ASCE 7. The seismic forces are estimated in two orthogonal directions accounting for accidental eccentricity of 5% of the building dimension perpendicular to the direction of the applied load. Wind loads were also considered in the design, but the seismic load combinations governed the design of the structural components.

The beams were designed as T-sections following ACI 318-14 (Section 18.6). The dimensions of the beams were set to allow the beam-column joints to be considered as confined per ACI 318-14 (Section 18.6.2.1), which requires the beam width be at least 75 percent of the column width. This last criterion governed the beam sizing. Four different beam designs (dimensions and reinforcing bar detailing) were defined for each floor level, including one external and

one internal beam design for each of two orthogonal directions. In addition, the longitudinal and transverse reinforcement of the beams are adjusted every three stories. Table 5 and Table 6 summarize the design detailing for all interior and exterior beams, respectively. Columns were designed to meet the strong-column weak-beam design requirements. Table 7 shows the design detailing for the columns. The design of the joints was performed according to ACI 318-14 (Section 18.8.4.)

Building Modeling

Nonlinear finite element models of the building structure were developed in OpenSees. The concentrated hinge modeling approach was adopted to represent the inelastic response of the structural components since it is consistent with the force-deformation criteria defined in most current building standards and guidelines, such as ASCE 41, ATC-72-1 (2010), and Haselton et al. (2017b). A concentrated hinge model consists of an elastic element interior with two concentrated hinges at the ends where the inelasticity develops. Rotational zero-length springs are typically used to model the hinges. In these zero-length spring elements, a moment-rotation backbone curve was adopted, representing key characteristics of the response including effective stiffness (k_e) yield (M_y) and ultimate (M_c) strength, hardening (θ_p), and post-peak strength loss (θ_{pc}) as shown in Fig. 2a. For the TBI and LATBSDC building modeling, parameters used for modeling the hysteretic response were calibrated based on experimental results (Haselton et al. 2017b). An example hysteretic response to cyclic loading is shown in Fig. 2b, which follows the “option 1” criteria that is recommended in the ATC-72-1 (2010) in which cyclic deterioration is explicitly incorporated in the analytical model using the initial (monotonic) backbone curve as a reference envelope. In response to the comment. The beam-column joints were modeled with effective rigid offsets for the columns, following suggestions in ASCE 41. This modeling approach is also allowed in TBI and LATBSDC for buildings designed using capacity design philosophy. To assess the performance of the ASCE 7 code-compliant building per three PBSE standards/guidelines at two hazard levels, three nonlinear models were thus developed to reflect the modeling recommendations in ASCE 41, TBI, and LATBSDC.

The modeling parameters used to develop the ASCE 41 conforming finite element model defined in this study are taken from ACI 369.1 (2017) document. The ACI 369.1 document has improved the robustness of the modeling parameters for columns and beams and the document is the basis of an adapted version of the of the ASCE 41 document that is currently out for public comment. The modeling parameters used in the development of the finite element models that conform to the TBI and LATBSDC guidelines are calculated per the empirical equations proposed by Haselton et al. (2016). For all models in this paper, the rigid diaphragm assumption is considered according to the ASCE 7 because the building does not have any horizontal irregularity or vertical discontinuities for the seismic resistance elements. This assumption may cause uncertainty in the distribution of forces in various structural components. However, for concentrated plastic hinge model that is employed in this study, the rigid diaphragm assumption is not expected to have a significant impact on the analysis results. The base of the columns of the first story are modeled as a fixed in all directions so the foundation modeling is not included.

Analysis Methods

The nonlinear finite element analysis of the models consists of three steps. In the first step, the gravity loads are applied to the structural system in ten increments using a load control nonlinear static analysis. The equilibrium equations are solved using the Newton-Raphson algorithm. In the second step, an eigenvalue analysis is performed to determine the periods of vibration, mode shapes, and mass participation factors for the building models. Rayleigh damping is assigned to the building model as proportional to the mass and initial stiffness, at the first natural frequency of vibration and at a mode that achieves 95% mass participation. In the third step, the nonlinear dynamic response history analysis is performed, where the Newmark time-integration method is used to solve the equations of motion with γ and α -factors equal to 0.5 and 0.25, respectively. P-Delta effects are considered in all analyses.

Eleven ground motion records are selected following the suggestions in Haselton et al. (2017a), which are following the procedures in ASCE 7. The ground motions are selected from the PEER NGA West II database and scaled to match the MCE_R hazard level for the site under consideration. The ground motions were scaled to the 43-year return period ground shaking intensity hazard level for the serviceability assessments. Two perpendicular components of each ground motion are applied simultaneously in the longitudinal and transverse direction of the building. Fig. 3Figure shows the scaled response spectrum of the all ground motion, median and the MCE_R target spectrum. Table 8 summarizes the selected ground motions details.

RESULTS

This section presents the results of the performance assessments of the building using the three different documents discussed in this paper. The assessment results according to the performance criteria described in each guideline are compared for two performance levels, including the Collapse Prevention at the MCE_R hazard level and Immediate Occupancy at the 43 -year return period ground shaking, i.e., serviceability. Table 9 presents the periods and mass participation ratios for the first twelve modes of the nonlinear models developed per ASCE 41, TBI, and LATBSDC. The ASCE 41 model exhibits higher period than the TBI and LATBSDC models due to the larger stiffness reduction factors assigned to the ASCE 41 model.

Collapse Prevention Performance Level

Fig. 4 shows the roof drift ratio in both X- and Y-directions of the three structural models when subjected to the 1952 Kern County earthquake record from the Taft Lincoln School station (earthquake 3 in Table 8). Fig. 4a, for example, illustrates that ASCE 41 building model exhibits peak roof drift ratios in the X-direction that are 65% larger than the ones observed for the other two guidelines, which show closer peak roof drift ratio values. In addition, the ASCE 41 building model exhibits residual drift ratio that is twice as large as the one measured from the analysis of the other two building models. However, the differences are not relevant in the Y-direction, as shown in Fig. 4b. The normalized story shear demands in the X- and Y-directions are shown in Fig. 5, where it can be seen that the LATBSDC show higher shear demands in Y- directions than the ASCE and TBI models. That higher shear demands in the LATBSDC model are mainly due to the higher flexural and shear rigidity factors used in this model (see Table 2).

Fig. 6 **Figure** shows the peak interstory drift ratio for the three building models subjected to all eleven earthquake ground motion records. In general, the computed peak interstory drift ratios for the ASCE 41 building model are larger than the peak interstory drift ratios from TBI and LATBSDC guidelines in both X- and Y-direction, which can be due to the lower effective stiffness used for the components in the ASCE 41 model than the ones used in the TBI and LATBSDC building models, even though the ASCE 41 model is defined using the higher expected strength and Young's Modulus material parameters. Recall that beam and column sizes are reduced at story 7, which explains the increase in interstory drift ratios from the sixth to seventh stories in the X-direction responses. However, this is not as pronounced in the Y-direction as it is in the X-direction.

The results in Fig. 6 can be used to compare to the acceptance criteria limits proposed by different guidelines with respect to peak interstory drift ratios. With respect to TBI and LATBSDC, the peak interstory drift ratios observed do not exceed the drift limits of 3%. ASCE 41 does not set explicit limits for the peak interstory drift ratio. However, ASCE 7 does specify that the peak interstory drift ratios cannot exceed 1.25 times the peak values interstory drift ratio values shown in Table 12.12.1, which would set the limit to 3.75% for the MCE_R hazard level assessment. Comparison of the ASCE 41 model responses with this ASCE 7 limit shows that peak interstory drift ratios did not exceed the ASCE 7 design criteria.

For the envelope of the peak interstory drift ratio for all eleven earthquakes in the X- and Y-directions, it can be seen that the ASCE 41 model exhibits the largest peak interstory drift ratios of about 5% in both directions, due to the lower effective stiffness of the components. The shape of the envelope in the Y-direction in a "Christmas tree" shape is typically observed in the literature for mid- to high-rise buildings with similar story stiffness along the height of the building. In the X-direction, however, it can be observed that the peak interstory drift ratios occur at story seven, which is the story in which the beam and column sizes are reduced. The results reveal that the envelope drift ratio of the LATBSDC model is 4.6%, which is slightly greater than the limit set by the LATBSDC procedure, i.e. 4.5%, in both X- and Y-directions. However, for the TBI building model, the peak values are lower than the 4.5% limit. Note, as mentioned above, that both ASCE 41 and ASCE 7 do not have specific limits for this criterion.

The TBI and LATBSDC guidelines provide acceptance criteria limits for the residual interstory drift ratios. The limits for the mean and envelope residual drift ratios are 1.0% and 1.5%, respectively. Fig. 7 shows the mean and the envelope residual drift ratio demands for the eleven ground motion responses in the X- and Y-directions. The results show that mean value in the X-direction exceeds the acceptance criteria limit for both TBI and LATBSDC. In addition, the envelope of the residual drift ratios greatly exceeds the limits proposed by the TBI and LATBSDC guidelines. Needless to say that the deformation and force demands computed in this study do not consider the impact of modeling uncertainty (Alam and Barbosa, 2018), and these results could be subject to changes if other modeling approaches or software packages are employed.

In addition to the global acceptance criteria, the deformation demands in the components of each of the nonlinear models are compared against the acceptance criteria in ASCE 41. Fig. 8. shows the mean of the peak rotation of the columns, and Fig. 9 and

Figure Fig. 10 show the mean of the peak rotation of the beams in X-direction, and Y-direction, respectively. Results in Fig. 10 show that the mean of the peak rotation of the columns from all models are significantly lower than the CP acceptance criteria proposed by ASCE 41, which range between 0.035-0.047 rad depending on the column axial load and section properties along the height of the building. For the beams, in both directions, the mean of the peak rotations does not exceed the CP acceptance criteria of the ASCE 41, which range between 0.04-0.05 rad, depending on the section properties.

Serviceability Performance Level

For the serviceability performance level, Fig. 11 shows the mean of the peak interstory drift ratios in the X- and Y-directions. For the TBI and LATBSDC models, at all stories, the drift ratios are lower than the acceptance criteria proposed by these guidelines, which is 0.5 %. Even though the ASCE 41 demands are higher than those obtained for the other two guidelines, it is worth noting that there is no specific criteria defined in this document ASCE 41 for limits on interstory drift ratios.

At the component level, TBI and LATBSDC documents propose that the hinge responses be compared to the limits for the immediate occupancy. The mean of the peak rotation of the columns are presented in Fig. 12. Fig. 13 and Fig. 14 show the mean of the peak rotation of the beams in the X- and Y-directions, respectively. Results indicate that the hinge rotation demands of the structural components are less than the IO limits acceptance criteria proposed by ASCE 41, which range between 0.005-0.006 rad for columns studies in these models and 0.008-0.01 rad for the beams analyzed.

CONCLUSIONS

In this study, a 12-story reinforced concrete special moment frame building is designed according to the ASCE 7 and ACI 318-14 for a far-field site located in Los Angeles, California. The building is assessed following the modeling recommendations and acceptance criteria in three different PBSE standards/guidelines, including ASCE 41, TBI, and LATBSDC. The performance assessments are conducted for the Collapse Prevention performance level at the MCE_R hazard level and Immediate Occupancy at the 43-year return period ground motion, i.e., serviceability performance level. Three-dimensional nonlinear finite element models were developed using OpenSees, in which concentrated hinge models were adopted to represent the nonlinear response of beams and columns. Three distinct models were developed following the modeling recommendations of each of the PBSE documents used. For all building models, a rigid diaphragm assumption was considered. Rayleigh viscous damping was assigned to the finite element models following the recommendations of each standard and guideline. The models were subjected to eleven bi-directional ground motion records selected to match the MCE_R target response spectrum for the site.

The serviceability performance level results indicate that mean of the interstory drift ratio meet the global acceptance criteria in TBI and LATBSDC guidelines. In addition, all components of the building had rotation demands that were less than the Immediate Occupancy acceptance criteria in ASCE 41.

The assessment results at the MCE_R hazard level indicate that the ASCE 7 code compliant building meets the acceptance criteria of the mean interstory drift ratio for TBI and LATBSDC guidelines. However, the mean of the residual drift ratios slightly exceeds the TBI and LATBSDC acceptance criteria in the 7th story. Results also exceed the peak residual drift limits per TBI and LATBSDC. All columns and beams in both directions exhibited rotation demands less than the ASCE 41 Collapse Prevention acceptance criteria.

The findings of this study indicate that the design of the building would need to be revised according to the TBI and LATBSDC guidelines in order to satisfy the interstory drift and residual drift ratio limits. This updated building design could be achieved by increasing the stiffness and strength of the building. This finding indicates that the building designed per TBI and LATBSDC would need to have a different design, when compared to the ones that would be obtained if the buildings are designed per ASCE 7 and checked using ASCE 41. The question that naturally arises is which building design would ultimately satisfy the performance objective for new buildings, which is a low probability of collapse, i.e. equal or less than 10% for a risk category II building per ASCE 7 at an MCE_R event. Future studies

should investigate the collapse probability of buildings designed per these different PBSE standards/guidelines to compare the collapse safety delivered by each document. The outcome of this research will help practicing engineers as well as code developers to make more informed decisions in designing new buildings or in developing future edition of the standards and guidelines.

REFERENCES

- ACI Committee 369.1, 2017, “Standard Requirements for Seismic Evaluation and Retrofit of Existing Concrete Buildings and Commentary” Version for Public Discussion Draft, American Concrete Institute, Farmington Hills, MI.
- ACI Committee 374.3, 2016, “Guide to Nonlinear Modeling Parameters for Earthquake-Resistant Structures” American Concrete Institute, Farmington Hills, MI.
- ACI Committee 318-14, 2014, “Building Code Requirements for Reinforced Concrete ACI 318-14 and Commentary,” American Concrete Institute, Farmington Hills, MI
- Alam, M.S. and Barbosa, A.R., 2018, “Probabilistic seismic demand assessment accounting for finite element model class uncertainty: Application to a code-designed URM infilled reinforced concrete frame building.” *Earthquake Engineering & Structural Dynamics*, Vol. 47 Issue 15, pp 2901-2920, DOI: 10.1002/eqe.3113
- ASCE 7-16, 2016, Minimum Design Loads for Buildings and Other Structures Including Supplement 1, American Society of Civil Engineers, Reston, VA.
- ASCE/SEI 41-17, 2017, “Seismic Evaluation and Upgrade of Existing Buildings,” American Society of Civil Engineers, Reston, Virginia. Public Comment Edition available through the American Society of Civil Engineers.
- PEER/ATC-72-1, 2010, “Modeling and acceptance criteria for seismic design and analysis of tall buildings,” Pacific Earthquake Engineering Research Center, Berkeley, CA, and Applied Technology Council, Redwood City, CA,
- CSI, 2013, ETABS User Manual (v13.1.5). Computer and Structures, Berkeley, CA.
- LATBSDC, 2014, “An Alternative Procedure for Seismic Analysis and Design of Tall Buildings Located in the Los Angeles Region,” Los Angeles Tall Building Structural Design Council, Los Angeles, CA.
- Haselton, C. B.; Baker, J. W.; Stewart, J. P.; Whittaker, A. S.; Luco, N.; Fry, A.; Hamburger, R. O.; Zimmerman, R. B.; Hooper, J. D.; Charney, F. A.; and Pekelnicky, R. G., 2017a, “Response history analysis for the design of new buildings in the NEHRP provisions and ASCE/SEI 7 standard: Part I - Overview and specification of ground motions,” *Earthquake Spectra* V. 33, No. 2, pp. 373–395.
- Haselton, C.B.; Fry, A.; Hamburger, R.O.; Baker, J.W.; Zimmerman, R.B.; Luco, N.; Elwood, K.N.; Hooper, J.D.; Charney, F.A.; Pekelnicky, R.G.; and Whittaker, A.S., 2017b, “Response History Analysis for the Design of New Buildings in the NEHRP Provisions and ASCE/SEI 7 Standard: Part II - Structural Analysis Procedures and Acceptance Criteria. *Earthquake Spectra*, V. 33, No. 2, pp. 397-417.
- Haselton, C. B.; Liel, A. B.; Taylor-Lange, S. C.; Deierlein, G. G., 2016, “Calibration of Model to Simulate Response of Reinforced Concrete Beam-Columns to Collapse,” *ACI Structural Journal*, V. 113, No. 6, pp.1141.
- Haselton, C.B.; Liel, A.B.; Taylor Lange, S.; and Deierlein, G.G., 2008. “Beam-Column Element Model Calibrated for Predicting Flexural Response Leading to Global Collapse of RC Frame Buildings”, *PEER Report 2007/03*, Pacific Earthquake Engineering Research Center, University of California, Berkeley, California.
- Ibarra, L. F.; Medina, R. A.; and Krawinkler, H., 2005, “Hysteretic Models that Incorporate Strength and Stiffness Deterioration,” *Earthquake Engineering & Structural Dynamics*, V. 34, No. 12, pp. 1489-1511.
- McKenna, F., Scott, M. H., and Fenves, G. L. 2009, “Nonlinear finite-element analysis software architecture using object composition,” *Journal of Computing in Civil Engineering*, V.24, No. 1, pp. 95-107.
- Moehle, J. P.; Hooper, J. D.; and Lubke, C. D., 2016, “Seismic Design of Reinforced Concrete Special Moment Frames: A Guide for Practicing Engineers” National Institute of Standards and Technology, Gaithersburg, MD.
- Tall Buildings Initiative, 2010, “Guidelines for performance-based seismic design of tall buildings,” Pacific Earthquake Engineering Research Center.

Table 1— Material over-strength factors convert nominal to expected material strength

Material	ASCE 41	TBI	LATBSDC
Concrete (ultimate compressive)	1.5	1.3	1.3
Reinforcing Steel	1.25	1.17	1.17

Table 2— Recommended flexural and shear rigidity factors

Component	ASCE 41		TBI		LATBSDC	
	Flexural Rigidity	Shear Rigidity	Flexural Rigidity	Shear Rigidity	Flexural Rigidity	Shear Rigidity
Beams	$0.30 E_c I_g$	$0.40 E_c A_w$	$0.50 E_c I_g$	$0.417 E_c A_w$	$0.35 E_c I_g$	$1.00 E_c A_w$
Columns	$0.30\text{-}0.48 E_c I_g$	$0.40 E_c A_w$	$0.50 E_c I_g$	$0.417 E_c A_w$	$0.70 E_c I_g$	$1.00 E_c A_w$

Table 3— Serviceability acceptance criteria

	ASCE 41*	TBI	LATBSDC
Global Limits	None	Story drift < 0.5%	Story drift < 0.5%
<i>Nonlinear Dynamic Response Analysis:</i>			
Deformation-controlled actions			
Demand	Max for $10 \geq n \geq 3$ GM Mean for $n \geq 10$ GM	Max for $n \geq 3$ GM Mean for $n \geq 7$ GM	Max for $n \geq 3$ GM Mean for $n \geq 7$ GM
Capacity	see ASCE 41 for IO criteria	ASCE 41 IO criteria	ASCE 41 IO criteria

* ASCE 41 BPON uses Life Safety at the DBE hazard level. For comparison purposes, this table assumes Immediate Occupancy at 50% in 30 years.

Table 4— Collapse prevention acceptance criteria

	ASCE 41	TBI	LATBSDC
Global Criteria			
Peak transient drift	None	Mean < 0.030 Max < 0.045	Mean < $0.03 \kappa_i$ Max < $0.045 \kappa_i$ ($\kappa_i = 1.0$ for Risk Category II)
Residual drift	None	Mean < 0.010 Max < 0.015	Mean < $0.01 \kappa_i$ Max < $0.015 \kappa_i$
Loss in story strength	None	< 20% of initial strength	< 20% of initial strength
Deformation-controlled actions			
Demand	- Max for ≤ 3 ground motions - Mean for ≥ 10 ground motions	Any response history analysis	Mean value
Capacity	See CP criteria from Tables in ASCE 41 Chapter 10	Ultimate deformation capacity ASCE 41 CP criteria or validated analytical models	κ_i * ASCE 41 CP criteria $\kappa_i = 1.0$ for Risk Category II

Table 5— Design details for the interior beams (1 in.=2.54cm)

Story 1-3	Dimensions (in.)			Longitudinal steel		Transverse steel
	b _w	h	b _f			
X- direction	24	28	90	10 #9	top	4 leg #4 @ 6"
				6 #8	bottom	
Y- direction	24	28	60	8 #8	top	4 leg #4 @ 5"
				6 #8	bottom	
Story 4-6	Dimensions (in.)			Longitudinal steel		Transverse steel
	b _w	h	b _f			
X- direction	24	28	90	8 #9	top	4 leg #4 @ 6"
				6 #8	bottom	
Y- direction	24	28	60	8 #8	top	4 leg #4 @ 6"
				6 #8	bottom	
Story 7-9	Dimensions (in.)			Dimensions (in.)		Dimensions (in.)
	b _w	h	b _f			
X- direction	22	26	90	8 #8	top	3 leg #4 @ 5.5"
				6 #7	bottom	
Y- direction	22	26	60	8 #7	top	3 leg #4 @ 5"
				6 #7	bottom	
Story 10-12	Dimensions (in.)			Longitudinal steel		Transverse steel
	b _w	h	b _f			
X- direction	22	26	90	8 #8	top	3 leg #4 @ 5"
				6 #7	bottom	
Y- direction	22	26	60	6 #7	top	3 leg #4 @ 5"
				4 #7	bottom	

Table 6— Design details for exterior beams (1 in.=2.54cm)

Story 1-3	Dimensions (in.)			Longitudinal steel		Transverse steel
	b _w	h	b _f			
X- direction	24	28	54	8 #9	top	4 leg #4 @ 6"
				6 #8	bottom	
Y- direction	24	28	44	8 #8	top	4 leg #4 @ 5.5"
				6 #8	bottom	
Story 4-6	Dimensions (in.)			Longitudinal steel		Transverse steel
	b _w	h	b _f			
X- direction	24	28	54	8 #8	top	3 leg #4 @ 6"
				6 #7	bottom	
Y- direction	24	28	44	8 #8	top	4 leg #4 @ 5.5"
				6 #8	bottom	
Story 7-9	Dimensions (in.)			Longitudinal steel		Transverse steel
	b _w	h	b _f			
X- direction	22	26	52	8 #8	top	3 leg #4 @ 5"
				6 #7	bottom	
Y- direction	22	26	42	8 #7	top	3 leg #4 @ 5"
				6 #7	bottom	
Story 10-12	Dimensions (in.)			Longitudinal steel		Transverse steel
	b _w	h	b _f			
X- direction	22	26	52	8 #8	top	3 leg #4 @ 5"
				6 #7	bottom	
Y- direction	22	26	42	6 #7	top	3 leg #4 @ 5"
				4 #7	bottom	

Table 7— Design details for Columns (1 in. = 2.54cm)

	Dimensions		Longitudinal Reinforcement				<i>Transverse steel*</i>
	Height in	Width in	Bar Size	No. of bars	A_{st} in ²	Ratio ρ	Adopted
Story 1-6	32	32	9	16	16.0	0.016	4 Leg # 5 @ 4.5 in
Story 4-6	32	32	9	12	12.0	0.012	4 Leg # 5 @ 5 in
Story 7-12	28	28	8	12	9.48	0.012	4 Leg # 5 @ 4.5 in

* Transverse reinforcements are closed hoops.

Table 8— Information on the earthquake records

#	Earthquake Name	Year	Station Name	R_{rup}^1	Magnitude	Scale factor for MCE_R
1	"Imperial Valley-02"	1940	"El Centro Array #9"	6.09	6.95	2.05
2	"Kern County"	1952	"Santa Barbara Courthouse"	82.19	7.36	4.07
3	"Kern County"	1952	"Taft Lincoln School"	38.89	7.36	3.62
4	"Northern Calif-03"	1954	"Ferndale City Hall"	27.02	6.5	2.14
5	"Parkfield"	1966	"Cholame - Shandon Array #5"	9.58	6.19	4.41
6	"Borrego Mtn"	1968	"El Centro Array #9"	45.66	6.63	3.29
7	"San Fernando"	1971	"LA - Hollywood Stor FF"	22.77	6.61	3.01
8	"San Fernando"	1971	"Pacoima Dam (upper left abut)"	1.81	6.61	1.11
9	"Managua_ Nicaragua-01"	1972	"Managua_ ESSO"	4.06	6.24	2.73
10	"Managua_ Nicaragua-02"	1972	"Managua_ ESSO"	4.98	5.2	4.49
11	"Coalinga-01"	1983	"Parkfield - Fault Zone 3"	6.09	6.36	3.50

¹ Fault rupture distance.

Table 9— Periods of vibration and mass participation ratios for the first twelve modes

Mode	ASCE 41				TBI				LATBSDC			
	T (sec.)	Mass Participation			T (sec.)	Mass Participation			T (sec.)	Mass Participation		
		X	Y	Z		X	Y	Z		X	Y	Z
1	4.48	0.77	0.00	0.16	3.52	0.80	0.00	0.17	4.01	0.77	0.00	0.17
2	4.01	0.77	0.78	0.50	3.14	0.80	0.80	0.57	3.58	0.77	0.78	0.54
3	3.80	0.77	0.78	0.78	2.82	0.80	0.80	0.80	3.05	0.77	0.78	0.78
4	1.55	0.89	0.78	0.80	1.23	0.91	0.80	0.83	1.38	0.89	0.78	0.81
5	1.42	0.89	0.90	0.86	1.12	0.91	0.92	0.88	1.25	0.89	0.90	0.87
6	1.34	0.89	0.90	0.90	1.00	0.91	0.92	0.91	1.05	0.89	0.90	0.90
7	0.83	0.94	0.90	0.91	0.67	0.95	0.92	0.92	0.74	0.93	0.90	0.91
8	0.77	0.94	0.94	0.93	0.62	0.95	0.95	0.94	0.68	0.93	0.94	0.93
9	0.74	0.94	0.94	0.94	0.55	0.95	0.95	0.95	0.58	0.93	0.94	0.94
10	0.53	0.96	0.94	0.95	0.45	0.97	0.95	0.96	0.49	0.96	0.94	0.95
11	0.49	0.96	0.97	0.96	0.42	0.97	0.97	0.97	0.46	0.96	0.97	0.96
12	0.48	0.96	0.97	0.96	0.38	0.97	0.97	0.97	0.39	0.96	0.97	0.97

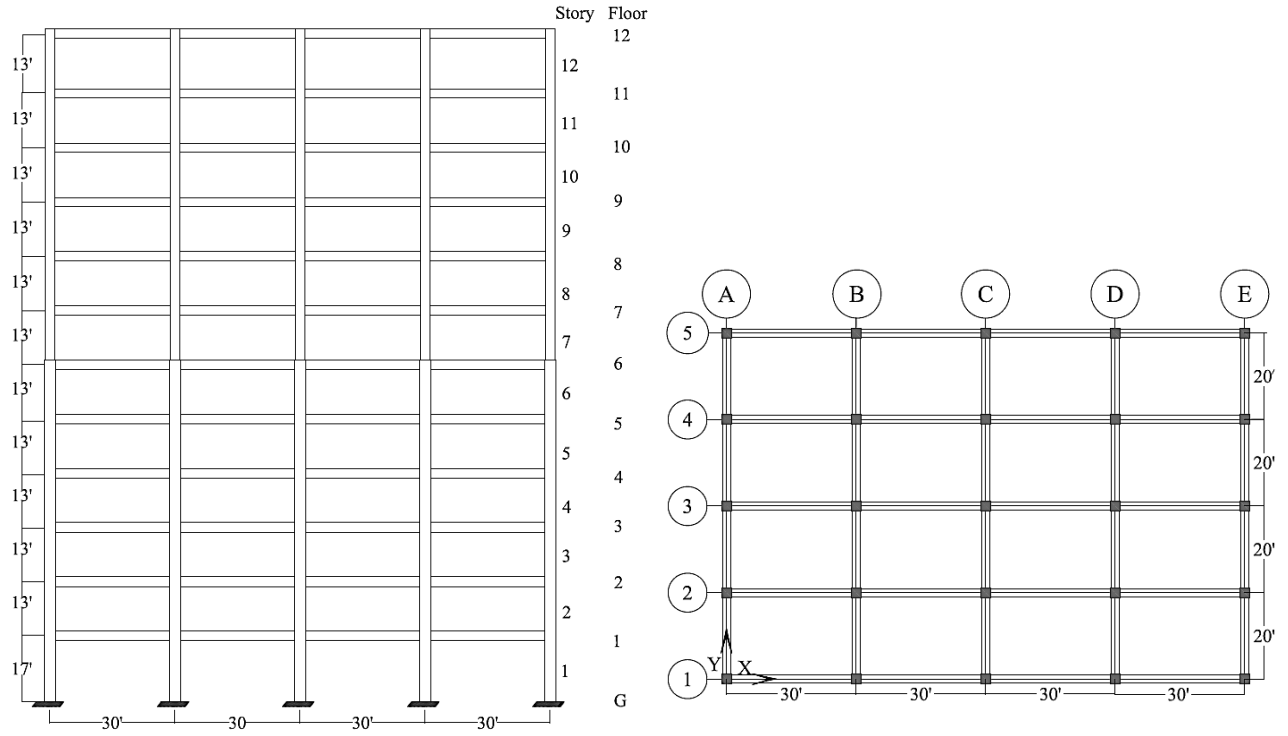


Figure 1— (a) elevation of the building, (b) plan view of building (1 ft. = 0.3 m)

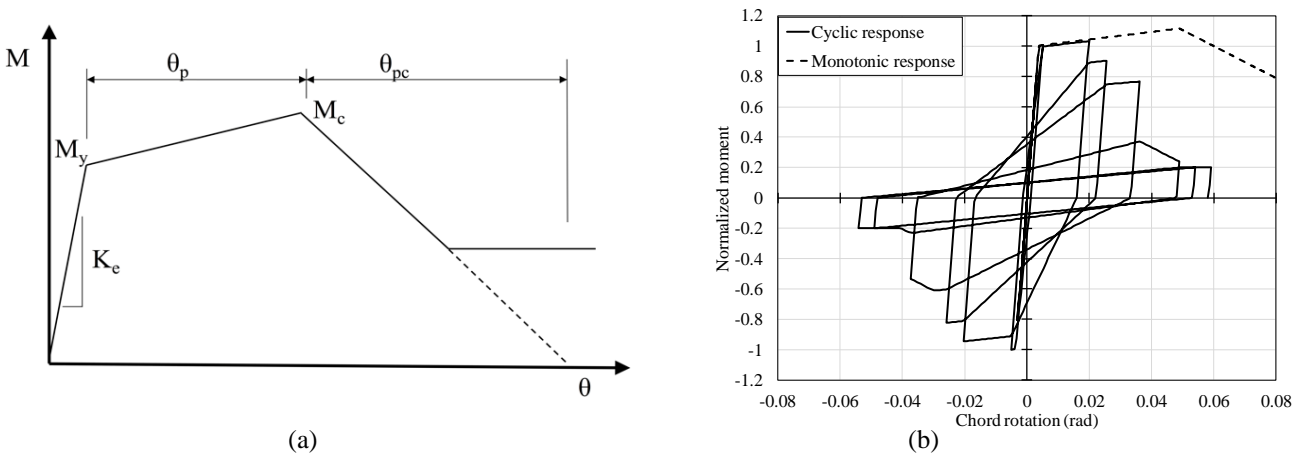


Figure 2— (a) Monotonic backbone curve, and (b) example cyclic behavior of component model

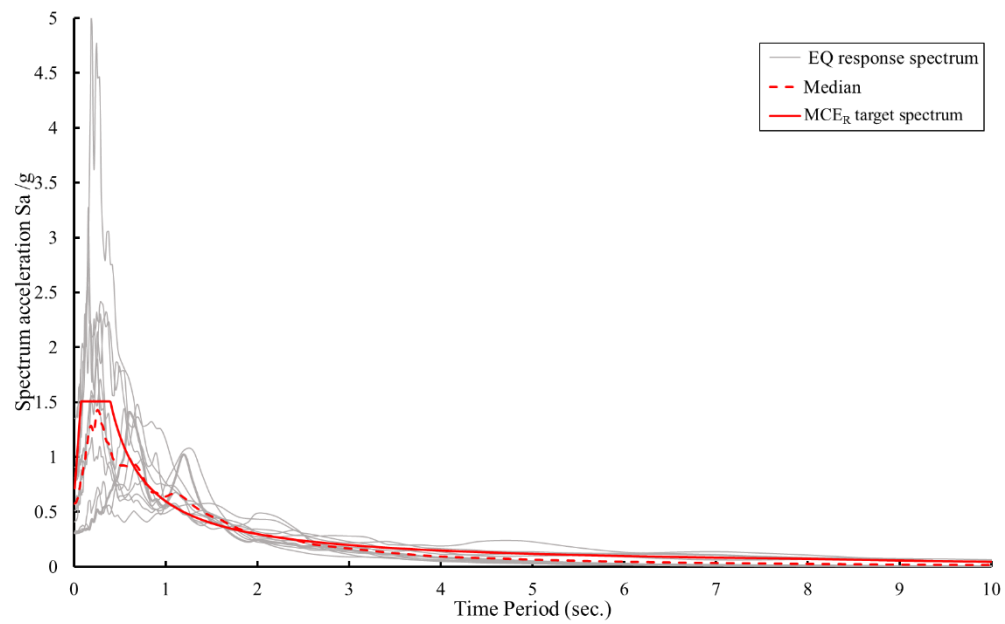


Figure 3— Scaled ground motion response spectra, mean of the scaled response spectra for all eleven ground motions listed in Table 8, and target response spectrum

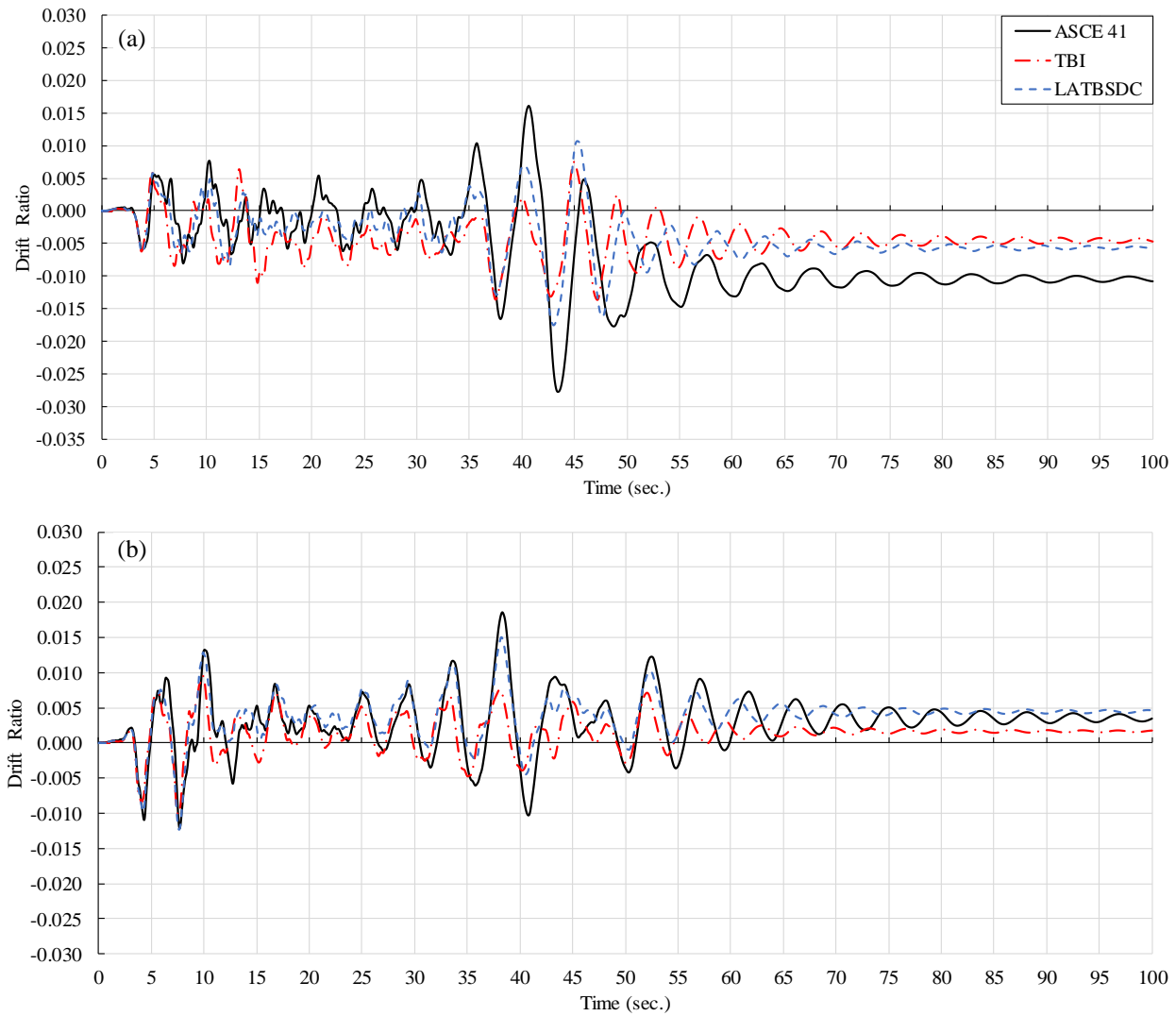


Figure 4— Roof drift ratio time-history responses for Earthquake 3 from Table 8 in (a) X-Direction, and (b) Y-Direction

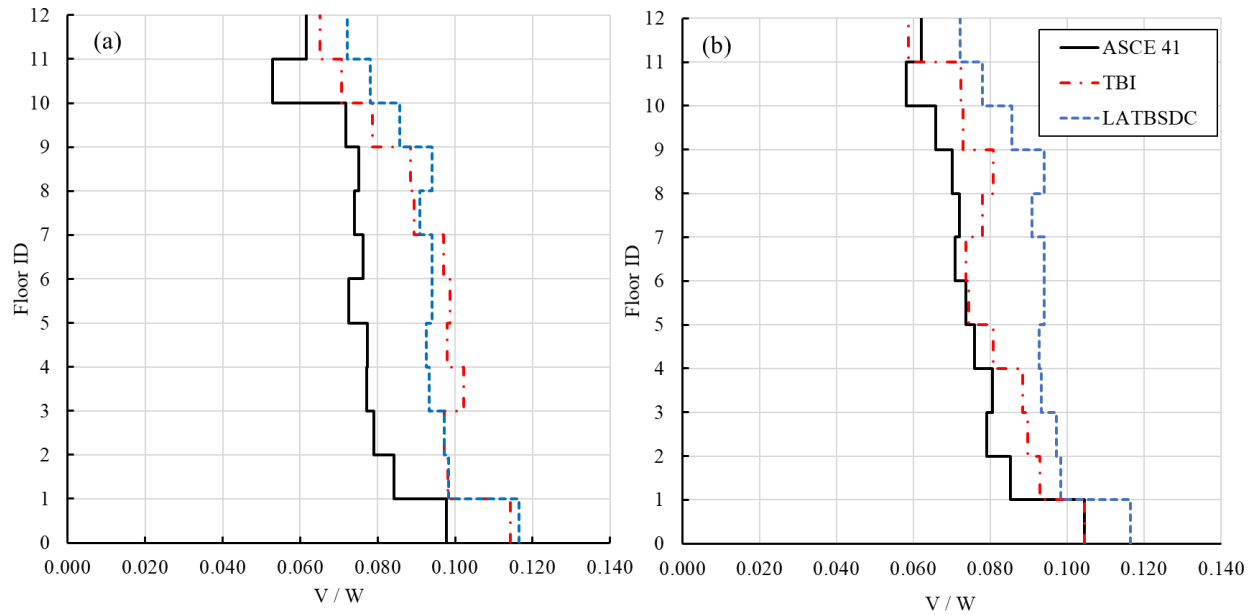


Figure 5— Normalized base shear from time-history analysis of Earthquake 3 from Table 8 in (a) X-Direction, and (b) Y-Direction

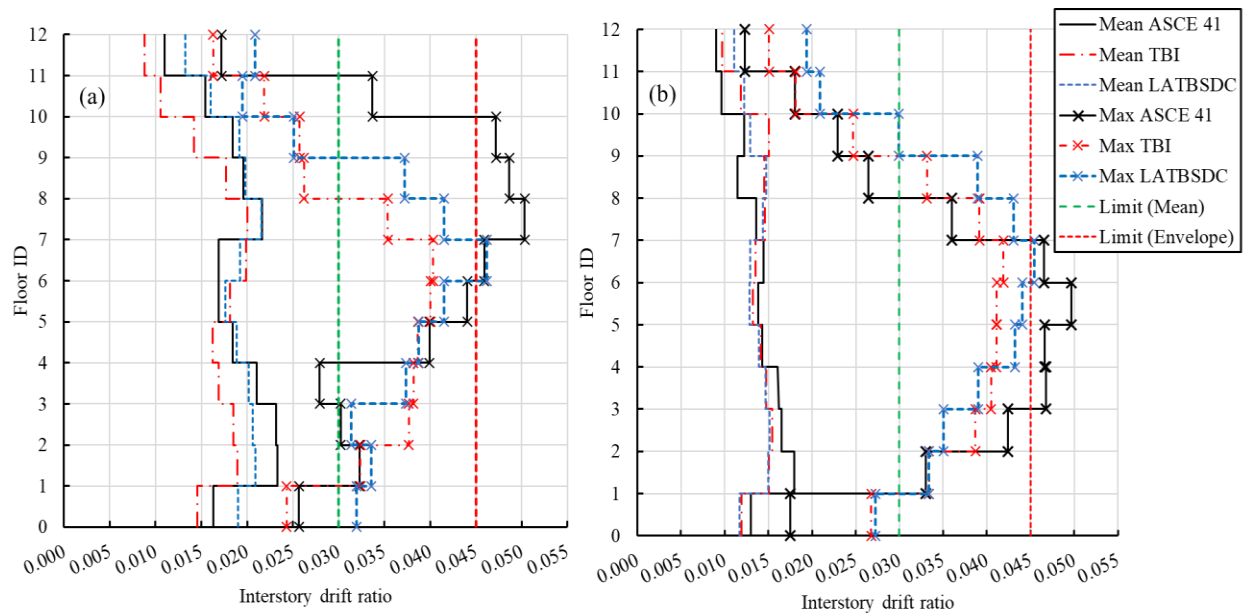


Figure 6— Peak interstory drift ratio of the archetype building per ASCE 41, TBI, and LATBSDC the MCE_R hazard level, in (a) X-Direction, and (b) Y-Direction

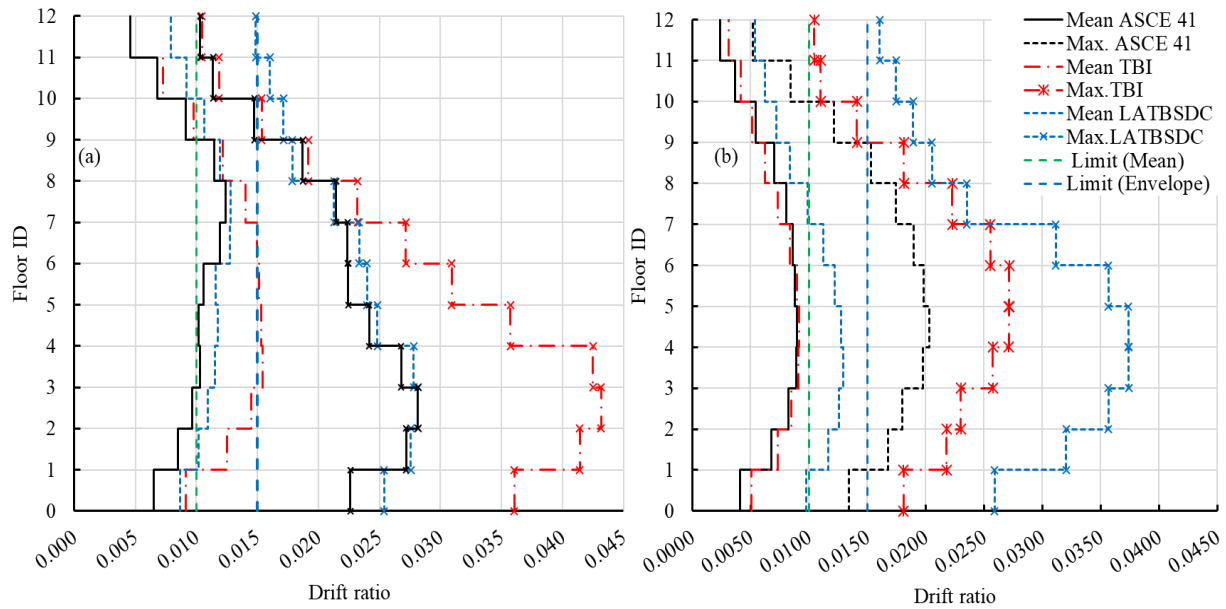


Figure 7— Residual interstory drift Ratio of the archetype building per ASCE 41, TBI, and LATBSDC the MCE_R hazard level, in (a) X-Direction, and (b) Y-Direction

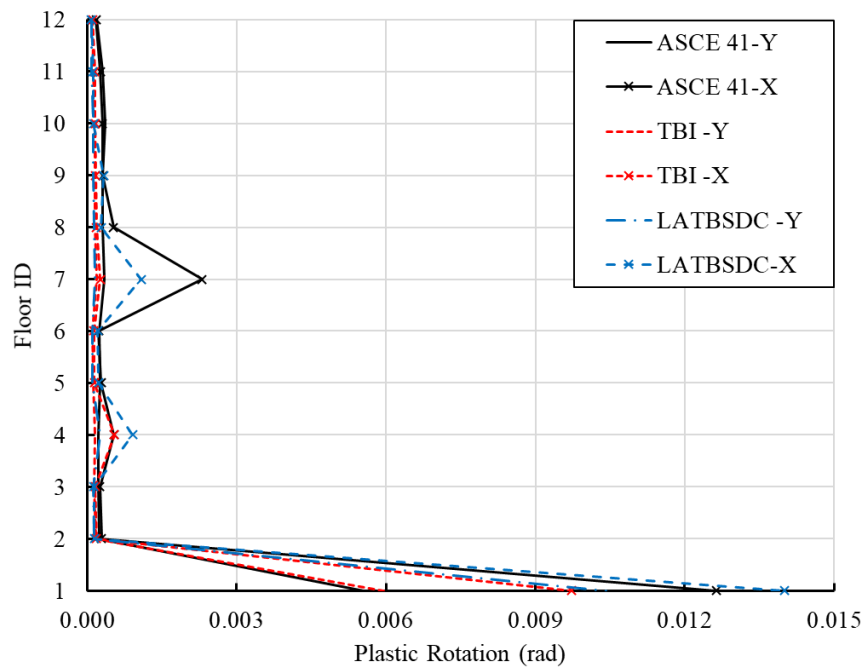


Figure 8— Mean peak rotation of columns for the archetype building per ASCE 41, TBI, and LATBSDC the MCE_R hazard level

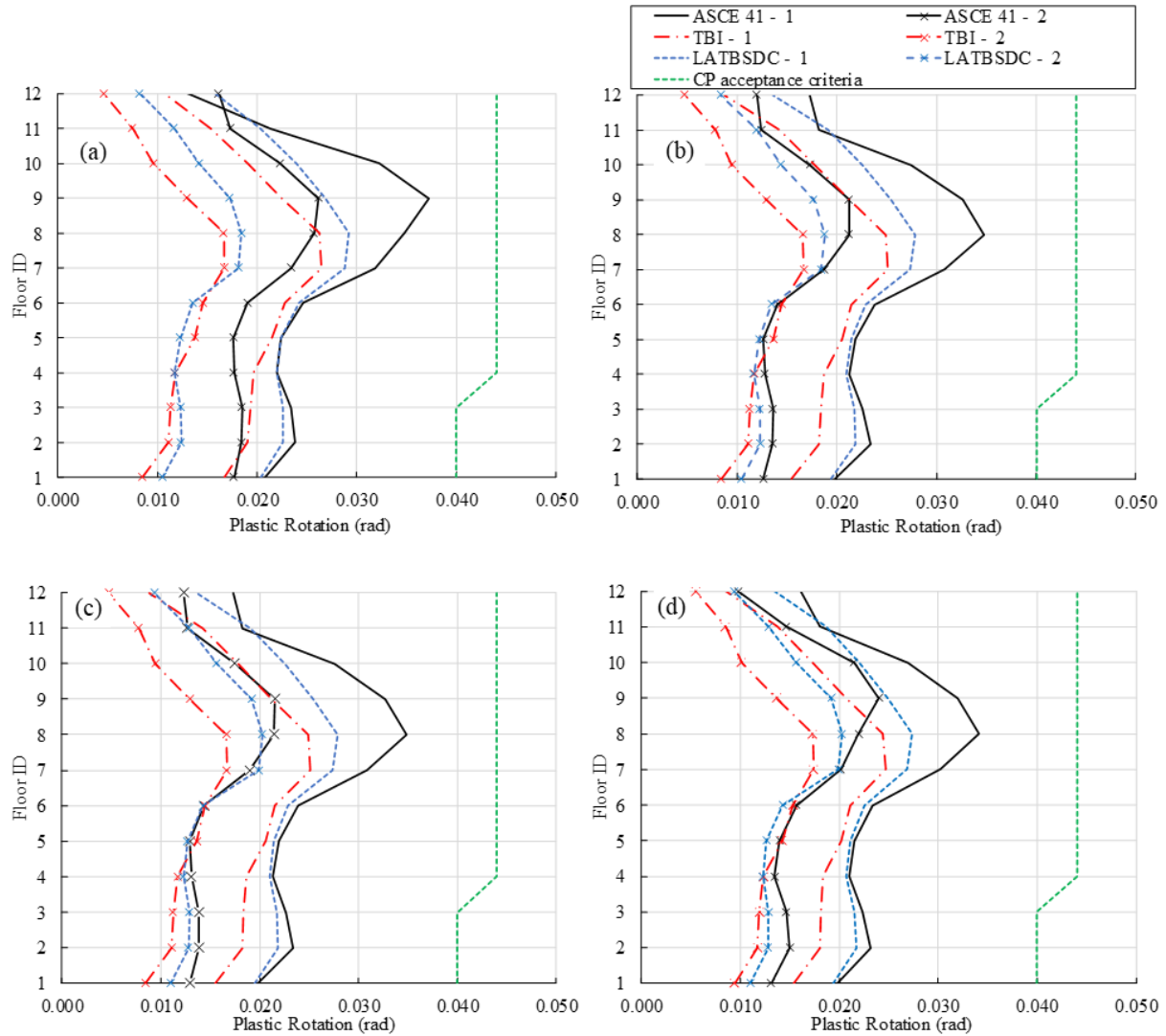


Figure 9— Mean peak rotation for beams in X-direction of the archetype building per ASCE 41, TBI, and LATBSDC for the MCE_R hazard level (a) Bay A-B, (b) Bay B-C, (c) bay C-D, (d) Bay D-E. In the legend, “- 1” and “- 2” correspond to beam left and right end of the beam in each bay

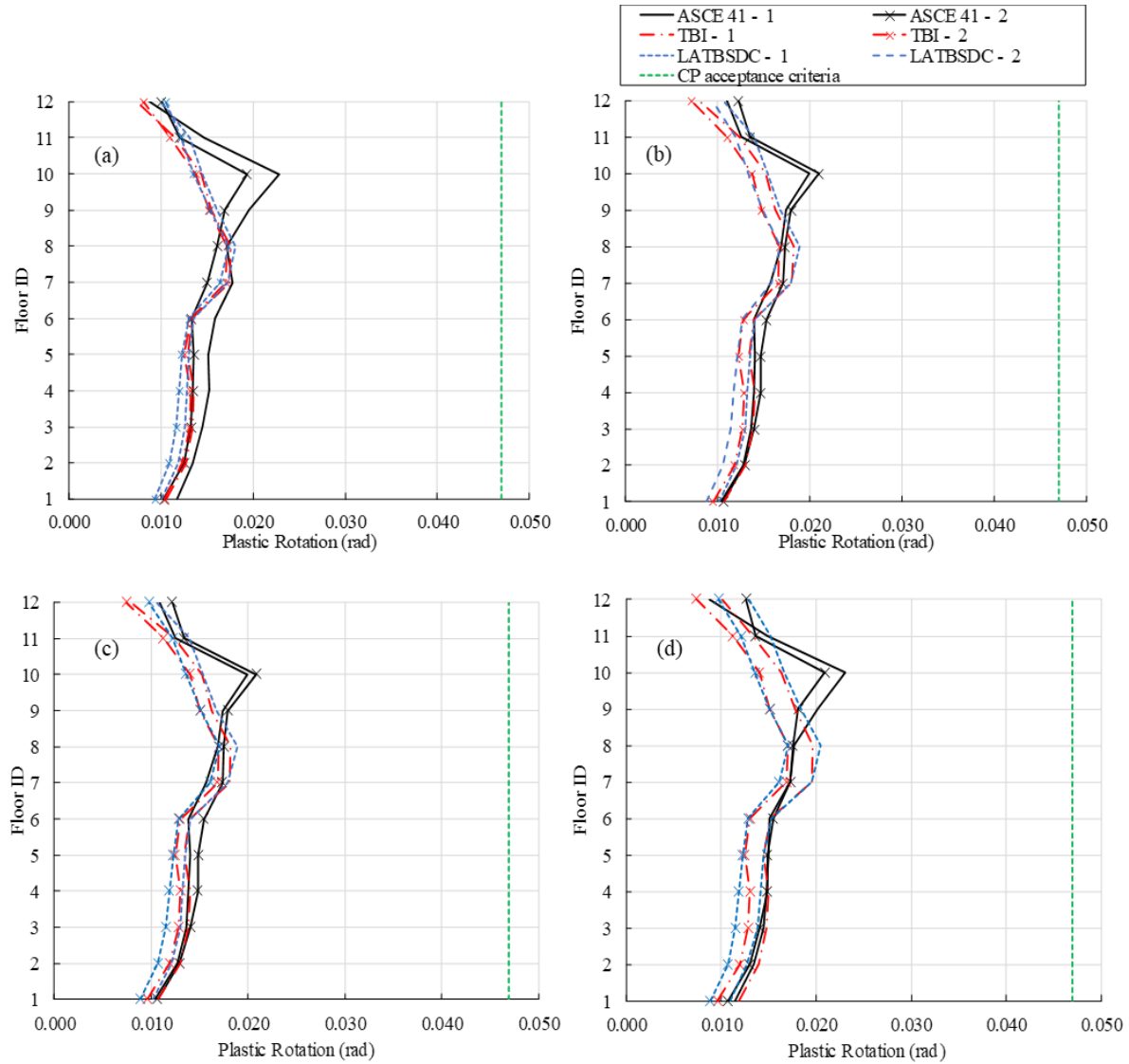


Figure 10— Mean peak rotation for beams in Y-direction of the archetype building per ASCE 41, TBI, and LATBSDC for the MCE_R hazard level (a) Bay A-B, (b) Bay B-C, (c) bay C-D, (d) Bay D-E. In the legend, “- 1” and “- 2” correspond to beam left and right end of the beam in each bay

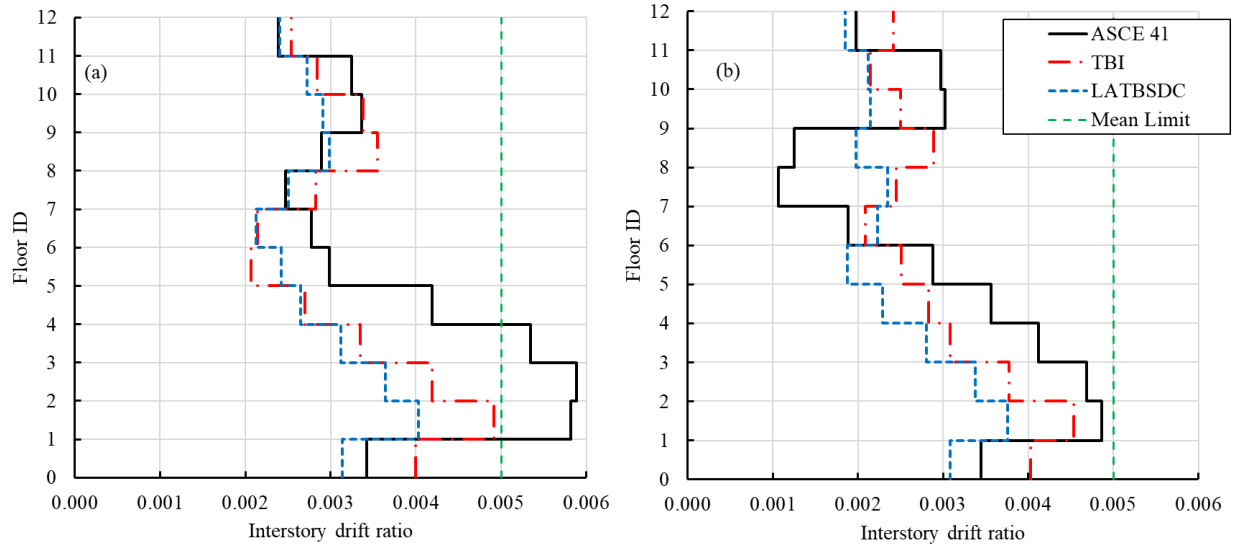


Figure 11— Mean peak interstory drift ratio of the archetype building per ASCE 41, TBI, and LATBSDC (serviceability level)

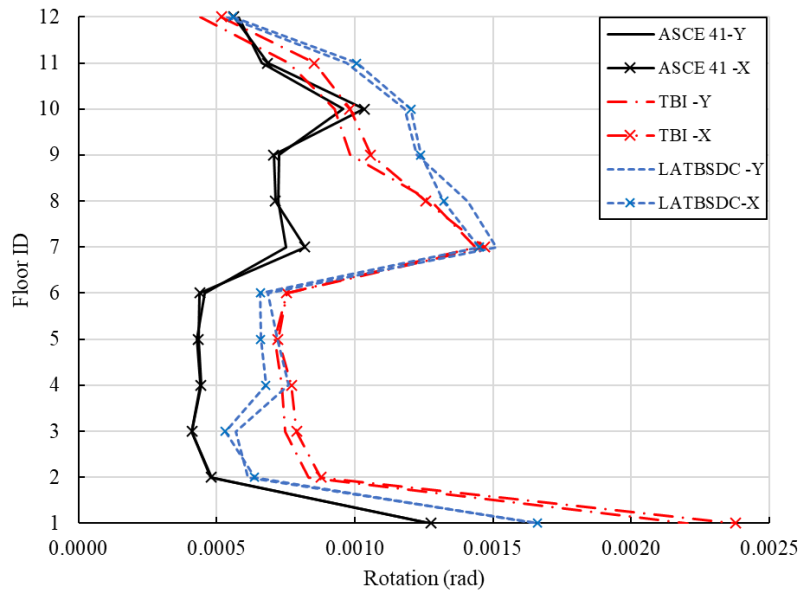


Figure 12— Mean peak rotation for columns of the archetype building per ASCE 41, TBI, and LATBSDC at serviceability level

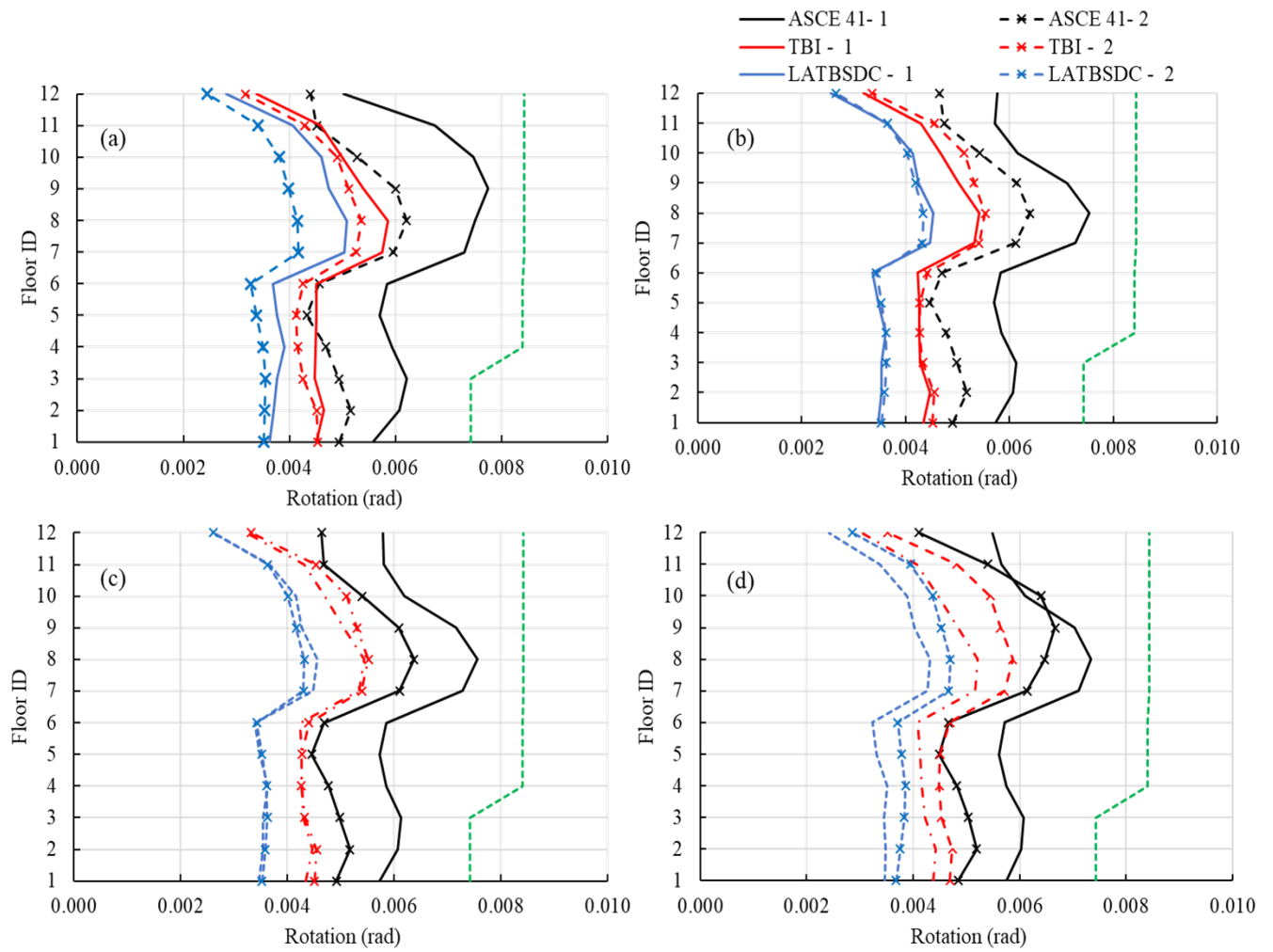


Figure 13— Mean of maximum rotation for beam in X-direction of the archetype building per ASCE 41, TBI, and LATBSDC at serviceability level, a) Bay A-B, b) Bay B-C, c) bay C-D, d) Bay D-E

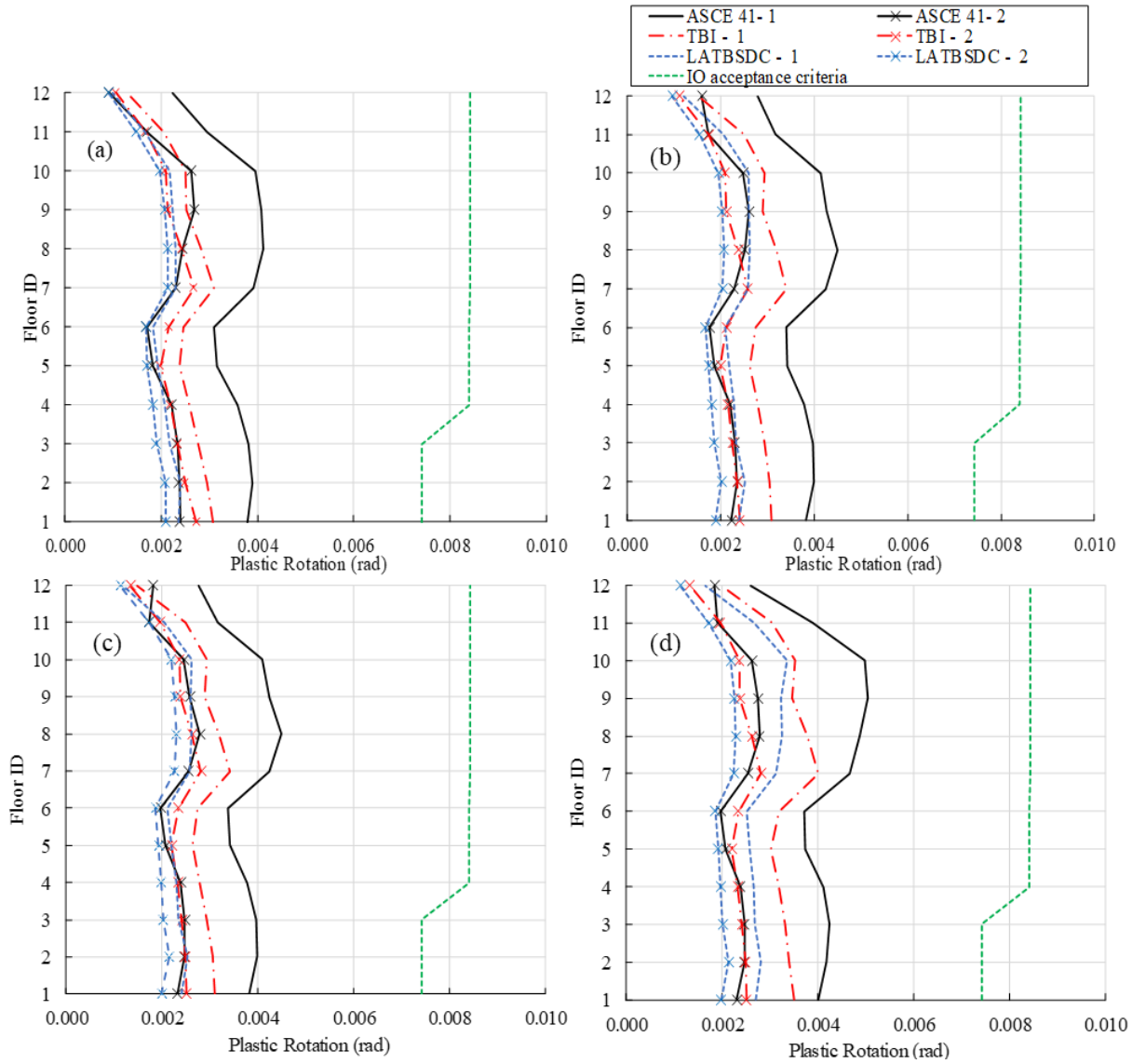


Figure 14— Mean of maximum rotation of the beams in Y-Direction of the archetype building per ASCE 41, TBI, and LATBSDC at serviceability level, a) Bay 1-2, b) Bay 2-3, c) bay 3-4, d) Bay 4-5